International Journal of Control, Automation and Systems 15(3) (2017) 1249-1258
http://dx.doi.org/10.1007/s12555-016-0010-1
ISSN:1598-6446 eISSN:2005-4092
http://www.springer.com/12555

# Auxiliary Particle Bernoulli Filter for Target Tracking

**Bo Li* and Jianli Zhao**

**Abstract:** Target tracking is a popular topic in various surveillance systems. As a data association free method, the Bernoulli filter can directly estimate target state from plenty of uncertain measurements. However, it is not obvious for existing Bernoulli filters to select proposal distribution with small variance of weights. To address this problem, a novel auxiliary particle (AP) Bernoulli filter and its implementation are proposed in this paper. We employ the AP method in the Bernoulli filtering framework in order to choose robust particles from a discrete distribution defined by an additional set of weights, which reflect the ability to represent measurements with high probability. Limitation to the number of particles, the promising particles are used to propagate by extracting indices. On the other hand, the particles without significant contribution to approximation are discarded. In such case, the computational complexity of this filter is reduced. With the unscented transform (UT), the dynamics of maneuvering target are effectively estimated. The simulation results show advantages in comparison to the standard Bernoulli filter for general target tracking.

**Keywords:** Auxiliary particle, Bernoulli filter, target tracking, weight.

## 1. INTRODUCTION

Target tracking is to sequentially estimate both state and number of the time-varying target with passive sensors from noise-corrupted measurements [1, 2]. So far, the target tracking continues to spur research interests in many surveillance applications, especially for the maneuvering target among plenty of ambiguous measurements [3–5]. However, the measurement uncertainty brings about unreliable estimations and unstable results. In the past decades, some scholars have studied target tracking with a great deal of success and many papers addressing the well established filtering algorithms have been published in the important international journals [6–8], such as the integrated probabilistic data association (IPDA), the joint probabilistic data association (JPDA), the multiple hypothesis tracking (MHT), etc. Nevertheless, these methods involve complex operation of data association when a large number of clutters appear around the true track or the detection probability of passive sensors is unsatisfactory [9]. The tracking performance would deteriorate because of the erratic estimations.

In order to reduce computational complexity, the Bernoulli filter has been derived in [10]. As for the general nonlinear non-Gaussian assumption, the particle filter (PF) method is more competent. Employed the tools of finite set statistics (FISST), the Bernoulli filter in [11] was under the assumption that the target state was a random finite set (RFS). Since it has no closed-form solution, the Bernoulli filter is usually achieved using the PF method. In [12], B. Ristic and S. Arulampalam discussed the implementation of the Bernoulli PF for observer control with excellent performance. For the sake of reduction in the number of particles, [13] presented the Bernoulli box-PF with more cost efficient. Subsequently, [14] described the multi-sensor Bernoulli filter in exact closed form to detect and track road-constrained targets using time different of arrival and frequency different of arrival measurements. In [15], a box-particle cardinality balanced multi-target multi-Bernoulli (CBMeMBer) filter was presented, which reduced both the number of particles and the running time under the similar accurate results. In [16], a Bernoulli PF was proposed for tracking maritime radiation source in the presence of measurement uncertainty, where the tracking performance under various conditions was still robust and effective. Among these filters, the basic idea is the sequential Monte Carlo (SMC) recursion on the basis of importance sampling (IS) [17]. This process limits tracking performance of the Bernoulli filter. As a result, the filter suffers from lacking of some efficient techniques for boosting its efficiency.

Traditional SMC method usually samples particles

Manuscript received January 7, 2016; revised July 19, 2016; accepted August 29, 2016. Recommended by Associate Editor Young Soo Suh under the direction of Editor Duk-Sun Shim. This journal was supported by the National Natural Science Foundation of China (No. 51679116), the Doctoral Scientific Research Foundation Guidance Project of Liaoning Province (No. 201601343), and the Scientific Research Project of Education Department of Liaoning Province (No. L2015230).

Bo Li and Jianli Zhao are with the School of Electronics and Information Engineering, Liaoning University of Technology, No. 169, Shiying Street, Guta District, Jinzhou 121001, China (e-mails: bo_li@yeah.net, 540088180@qq.com).
* Corresponding author.

based on the proposal distribution defined by their weights. It is important to ensure the variance of weights minimized in the process of the IS [18]. Once the weights with high variance rapidly degenerate with time, the associated particle can yield poor estimations. In this case, the resampling must be frequently performed, which further leads to increasing variance of weights. Therefore, the proposal distribution should be considered as a metrics of practical efficiency of the SMC method. However, it is not obvious to choose the proposal distribution for minimizing variance in the existing Bernoulli filters. To address this problem, one of the most prominent methods is the auxiliary particle (AP) implementation [19], where the particles are propagated from a discrete distribution defined by a set of weights that reflect the ability to express available measurements with high probability [20, 21]. In 2016, H. Chen and C.Z. Han proposed a new SMC implementation of the CBMeMBer filter [22]. Combined AP filtering method with progressive correction algorithm, the filter improves the solving accuracy of sampling distribution function. As we know, the filtering principle of the Bernoulli filter is essentially different from that of [20–22]. Especially, the decomposition method of the proposal distributions cannot be directly applicable to the Bernoulli filter, where the probability hypothesis density (PHD) and the prior density component are approximated respectively. Inspired by excellent performance of the AP implementation for target tracking, this paper presents a novel AP-Bernoulli filter and its implementation. It boosts tracking efficiency for the Bernoulli filter by providing the proposal distribution. The filter distinctly exhibits a new mechanism for choice of particles to propagate based on measurements to which they are assigned. More importantly, the filter has lower computational complexity because the effective sample size (ESS) is utilized to limit the number of particles, and the state estimates of the maneuvering target are estimated based on the unscented transform (UT).

The remainder of this note is organized as follows: In Section 2, the problem of the target tracking is briefly formulated. In Section 3, the principle of the standard Bernoulli filter is reviewed. In Section 4, we present the improvements of the proposed Bernoulli filter and illustrate its AP implementation. The numerical study is showed with results to verify tracking performance of the proposed filter in Section 5. In the last section, the conclusions are drawn by providing the future work.

## 2. PROBLEM FORMATION

Assume $n_k$ is the dimension of states in the space $\mathcal{X} \subseteq \mathbb{R}^{n_k}$, the target motion at time $k$ is modeled by:

$$\mathbf{x}_k = \mathbf{F}_{k|k-1}\mathbf{x}_{k-1} + \mathbf{\Gamma}_k \mathbf{v}_k, \tag{1}$$

where $\mathbf{F}_{k|k-1}$ is the state transition matrix, $\mathbf{\Gamma}_k$ is the state noise input matrix, $\mathbf{v}_k$ is the state noise vector with zero mean and variance $\mathbf{Q}_k$, and $\mathbf{x}_{k-1}$ is the target state vector at time $k-1$.

Assume $m_k$ is the number of measurements in the space $\mathcal{Z} \subseteq \mathbb{R}^{m_k}$, and the conventional measurement $\mathbf{z}_k$ in the set $\mathbf{Z}_k = \{\mathbf{z}_{1,k}, \cdots, \mathbf{z}_{m_k,k}\}$. The measurement model at time $k$ is given by the nonlinear equation [23–26]:

$$\mathbf{z}_k = h_k(\mathbf{x}_k) + \mathbf{w}_k, \tag{2}$$

where $\mathbf{w}_k$ is the measurement noise vector with zero mean and variance $\mathbf{R}_k$, and $h_k(\cdot)$ is a known deterministic mapping from $\mathcal{X}$ to $\mathcal{Z}$:

$$h_k(\mathbf{x}_k) = \text{atan2}(x_k, y_k), \tag{3}$$

where $\text{atan2}(\cdot)$ denotes the arctangent function with two arguments. The main idea is to gather the sign information of inputs and to return appropriate quadrant of computed angle in radians between the positive $x$-position of a plane and the point given in $x$-$y$ coordinates. Then, $h_k(x_k)$ can be considered as a four-quadrant inverse tangent function, taking values from $\mathcal{Z}$.

**Remark 1:** In general, the passive sensor cannot collect all measurements generated from targets due to the imperfect characteristics. It reports that there is a closed interval which contains the target originated measurement with the detection probability $p_D(\mathbf{x}_k)$. The false detections from clutters are independent of the target state, where the number of false alarms follows the Poisson distribution with the mean $\lambda$, and the prior probability is modeled by $c(\mathbf{z}_m)$. Therefore, $\mathbf{Z}_k$ is characterized by two sources of uncertainty: i) the additive Gaussian noise $\mathbf{w}_k$ has stochastic uncertainty; ii) the existence of false alarms and the absence of target originated detection have data association uncertainty.

## 3. STANDARD BERNOULLI FILTER

### 3.1. Filtering principle

As we know, the Bernoulli filter models the state of targets at time $k$ as a Bernoulli RFS in the set $\mathbf{X}_k$ for the nonlinear and non-Gaussian estimation of dynamic system. If the state of the target is given by a Bernoulli RFS, the Bernoulli filter can estimate two posteriors: the posterior probability of the target existence $q_{k|k} = P\{|\mathbf{X}_k| = 1|\mathbf{Z}_{1:k}\}$ and the posterior spatial probability density function (PDF) of the target state $s_{k|k}(\mathbf{x}_k) = p(\mathbf{x}_k|\mathbf{Z}_{1:k})$. The Bernoulli Markov process $X_k$ is completely specified by a pair $\left(q_{k|k}, s_{k|k}(\mathbf{x}_k)\right)$ and the associated PDF is defined as:

$$f(\mathbf{X}_k|\mathbf{Z}_{1:k}) = \begin{cases} 1 - p_{b,k|k-1}, & \mathbf{X}_k = \varnothing \\ p_{s,k|k-1}(\mathbf{x}_{k-1}) f_{k|k-1}(\mathbf{x}_k|\mathbf{x}_{k-1}), & \mathbf{X}_k = \{\mathbf{x}_k\} \\ 0, & |\mathbf{X}_k| \geq 2, \end{cases} \tag{4}$$

where $p_{b,k|k-1}$ and $p_{s,k|k-1}(\mathbf{x}_{k-1})$ are the probabilities of target birth and target survival, and $f_{k|k-1}(\mathbf{x}_k|\mathbf{x}_{k-1})$ is the target transition density from time $k-1$ to $k$.

Due to the Bernoulli filter propagation two quantities versus time, $\mathbf{X}_k$ can be characterized by the transitional PDF $f(\mathbf{X}_k|\mathbf{X}_{k-1})$:

$$f(\mathbf{X}_k|\mathbf{X}_{k-1}) = \begin{cases} 1-p_{b,k|k-1}, & \mathbf{X}_k=\varnothing,\ \mathbf{X}_{k-1}=\varnothing, \\ 1-p_{s,k|k-1}(\mathbf{x}_{k-1}), & \mathbf{X}_k=\varnothing,\ \mathbf{X}_{k-1}=\{\mathbf{x}_{k-1}\}, \\ p_{b,k|k-1}b_{k|k-1}(\mathbf{x}_k), & \mathbf{X}_k=\{\mathbf{x}_k\},\ \mathbf{X}_{k-1}=\varnothing, \\ p_{s,k|k-1}(\mathbf{x}_{k-1})f_{k|k-1}(\mathbf{x}_k|\mathbf{x}_{k-1}), & \mathbf{X}_k=\{\mathbf{x}_k\},\ \mathbf{X}_{k-1}=\{\mathbf{x}_{k-1}\}, \\ 0, & |\mathbf{X}_k|\geq 2, \end{cases} \tag{5}$$

where $b_{k|k-1}(\mathbf{x}_k)$ is the target birth density.

Conditioned upon the cardinality of $\mathbf{X}_k$, the likelihood function of $\mathbf{Z}_k$ is given by:

$$g_k(\mathbf{Z}_k|\mathbf{X}_k) = \begin{cases} L_c(\mathbf{Z}_k), & \mathbf{X}_k=\varnothing \\ L_c(\mathbf{Z}_k)\left(1-p_D+p_D\sum_{m=1}^{|\mathbf{Z}_k|}\frac{g_k(\mathbf{z}_m|\mathbf{x}_k)}{\lambda c(\mathbf{z}_m)}\right), & \mathbf{X}_k=\{\mathbf{x}_k\}, \end{cases} \tag{6}$$

where $g_k(\mathbf{z}_m|\mathbf{x}_k)$ is the likelihood of the single target, and $L_c(\mathbf{Z}_k)$ is the probability density of clutters, i.e.,

$$L_c(\mathbf{Z}_k) = e^{-\lambda}\prod_{m=1}^{|\mathbf{Z}_k|}\lambda c(\mathbf{z}_m). \tag{7}$$

Subsequently, we have the prediction equations of the Bernoulli filter:

$$q_{k|k-1} = p_{b,k|k-1}\left(1-q_{k-1|k-1}\right) + p_{s,k|k-1}(\mathbf{x}_k)\,q_{k-1|k-1}, \tag{8}$$

$$s_{k|k-1}(\mathbf{x}_k) = \frac{1}{q_{k|k-1}}\begin{pmatrix} p_{b,k|k-1}\left(1-p_{k-1|k-1}\right)b_{k|k-1}(\mathbf{x}_k) \\ +q_{k-1|k-1}\int p_{s,k|k-1}(\mathbf{x}_{k-1})f_{k|k-1}(\mathbf{x}_k|\mathbf{x}_{k-1}) \\ \times s_{k-1|k-1}(\mathbf{x}_{k-1})\,\mathrm{d}\mathbf{x}_{k-1} \end{pmatrix}, \tag{9}$$

$$q_{k|k} = \frac{q_{k|k-1}-q_{k|k-1}\Delta_k}{1-q_{k|k-1}\Delta_k}, \tag{10}$$

$$s_{k|k}(\mathbf{x}_k) = \frac{s_{k|k-1}(\mathbf{x}_k)}{1-\Delta_k}\left(1-p_D(\mathbf{x}_k)+p_D(\mathbf{x}_k)\sum_{m=1}^{|\mathbf{Z}_k|}\frac{g_k(\mathbf{z}_m|x_k)}{\lambda c(\mathbf{z}_m)}\right), \tag{11}$$

where the quantity $\Delta_k$ is given by:

$$\Delta_k = p_D(\mathbf{x}_k)\left(1-\sum_{m=1}^{|\mathbf{Z}_k|}\frac{\int g_k(\mathbf{z}_m|\mathbf{x}_k)\,s_{k|k-1}(\mathbf{x}_k)\,\mathrm{d}\mathbf{x}_k}{\lambda c(\mathbf{z}_m)}\right). \tag{12}$$

**Remark 2:** When the detection probability of sensor is $p_D(\mathbf{x}_k)=1$ and no false alarm is assumed, $\mathbf{Z}_k$ only contains the target originated measurements. At this time, we can find that $\lambda c(\mathbf{z}_m)$ is canceled out in both (11) and (12). The Bernoulli filter simplifies to conventional Bayes filter in terms of $p_{b,k|k-1}=0$ and $p_{s,k|k-1}(\mathbf{x}_{k-1})=1$.

### 3.2. Particle implantation

The general implementation of the Bernoulli filter is based on the SMC-based method, where a set of the weighted particles is recursively propagated as the approximation of the posterior density. The Bernoulli PF can approximate $s_{k|k}(\mathbf{x}_k)$ by a weighted particle set $\left\{\mathbf{x}_k^{(i)},\mathbf{w}_k^{(i)}\right\}_{i=1}^{N_k}$, where $\mathbf{x}_k^{(i)}$ is the state of the $i$th particle and $\mathbf{w}_k^{(i)}$ is related normalized weight, i.e., $\sum_{i=1}^{N_k}\mathbf{w}_k^{(i)}=1$. Then, $s_{k|k}(\mathbf{x}_k)$ is approximated as:

$$s_{k|k}(\mathbf{x}_k) = \sum_{i=1}^{N_k}\mathbf{w}_k^{(i)}\delta_{\mathbf{x}_k^{(i)}}(\mathrm{d}\mathbf{x}_k), \tag{13}$$

where $N_k$ is the total number of particles at time $k$ and $\delta_{\mathbf{x}_k^{(i)}}(\cdot)$ is the Dirac delta function concentrated at $\mathbf{x}_k^{(i)}$.

Regarding $q_{k-1|k-1}$ and $\left\{\mathbf{x}_{k-1}^{(i)},\mathbf{w}_{k-1}^{(i)}\right\}_{i=1}^{N_{k-1}}$ at time $k-1$, the recursion of the standard Bernoulli PF at time $k$ is summarized in Algorithm 1. Note that the predicted particles $\mathbf{x}_{s,k}^{(i)}$ and $\mathbf{x}_{b,k}^{(i)}$ as well as their weights $\mathbf{w}_{s,k|k-1}^{(i)}$ and $\mathbf{w}_{b,k|k-1}^{(i)}$ are based on the time-updated parameters. For each updated measurement, the normalized weight $\mathbf{w}_k^{(i)}$ should be computed again. By resampling $N_k$ times from the set $\left\{\mathbf{x}_{k|k-1}^{(i)},\mathbf{w}_{k|k-1}^{(i)}\right\}_{i=1}^{N_k}$, we can achieve $q_{k|k}$, $s_{k|k}(\mathbf{x}_k)$ and $\left\{\mathbf{x}_k^{(i)},\mathbf{w}_k^{(i)}\right\}$.

**Remark 3:** Note that the particle implementation of the Bernoulli filter is on the basis of the sequential IS method. It is important to minimize the variance of weights. If the degeneracy of weights would be avoided, the SMC method should take into account available measurements to drive particles into the region of probabilities. However, we hardly choose the proposal distributions $f_{k|k-1}\left(\mathbf{x}_k|\mathbf{x}_{k-1}^{(i)}\right)$ and $f_{k|k-1}\left(\mathbf{x}_k|\mathbf{x}_{b,k-1}^{(i)}\right)$ when drawing the particles $\mathbf{x}_{s,k}^{(i)}$ and $\mathbf{x}_{b,k}^{(i)}$. Then, the sampling operation must be performed frequently and effectively. Once the particles with high weights rapidly degenerate versus time, the error of dynamic estimates would further increase. The numbers $N_{s,k-1}$ and $N_{b,k-1}$ can cause higher computational complexity in practice.

**Algorithm 1:** Pseudo-code of standard Bernoulli filter

**Input:**

1. Given $q_{k-1|k-1}$, $\{\mathbf{x}_{k-1}^{(i)}, \mathbf{w}_{k-1}^{(i)}\}_{i=1}^{N_{k-1}}$, $\mathbf{Z}_{k-1}$ and $\mathbf{Z}_k$;

**Time update:**

2. Compute $q_{k|k-1}$:
   $q_{k|k-1}$
   $= p_{b,k|k-1}\left(1-q_{k-1|k-1}\right) + p_{s,k|k-1}\left(\mathbf{x}_{k-1}^{(i)}\right) q_{k-1|k-1}$;
3. for $i = 1$ to $N_{x,k-1}$
4. Draw survival particle $\mathbf{x}_{s,k}^{(i)}$: $\mathbf{x}_{s,k}^{(i)} \sim f_{k|k-1}\left(\mathbf{x}_k|\mathbf{x}_{k-1}^{(i)}\right)$;
5. Predict weight of survival particle $\mathbf{w}_{s,k|k-1}^{(i)}$:
   $\mathbf{w}_{s,k|k-1}^{(i)} = \frac{p_{s,k|k-1}q_{k-1|k-1}}{q_{k|k-1}}\mathbf{w}_{k-1}^{(i)}$;
6. end for
7. for $i = 1$ to $N_{b,k-1}$
8. Draw newborn particle $\mathbf{x}_{b,k}^{(i)}$:
   $\mathbf{x}_{b,k}^{(i)} \sim f_{k|k-1}\left(\mathbf{x}_k|\mathbf{x}_{b,k-1}^{(i)}\right)$;
9. Predict weight of survival particle $\mathbf{w}_{b,k|k-1}^{(i)}$:
   $\mathbf{w}_{b,k|k-1}^{(i)} = \frac{p_{b,k|k-1}\left(1-q_{k-1|k-1}\right)}{q_{k|k-1}N_{b,k-1}}$;
10. end for
11. Let $N_k = N_{s,k-1} + N_{b,k-1}$ and union of particles:
    $\left\{\mathbf{x}_{k|k-1}^{(i)}, \mathbf{w}_{k|k-1}^{(i)}\right\}_{i=1}^{N_k}$
    $= \left\{\mathbf{x}_{s,k}^{(i)}, \mathbf{w}_{s,k|k-1}^{(i)}\right\}_{i=1}^{N_{s,k-1}} \bigcup \left\{\mathbf{x}_{b,k}^{(i)}, \mathbf{w}_{b,k|k-1}^{(i)}\right\}_{i=1}^{N_{b,k-1}}$;

**Measurement update:**

12. for $\mathbf{z}_m \in \mathbf{Z}_k$
13. Compute $\Delta_k$:
    $\Delta_k = p_D\left(\mathbf{x}_k\right)\left(1 - \sum_{m=1}^{|\mathbf{Z}_k|}\sum_{i=1}^{N_k}\frac{g_k\left(\mathbf{z}_m|\mathbf{x}_{k|k-1}^{(i)}\right)}{\lambda c(\mathbf{z}_m)}\mathbf{w}_{k|k-1}^{(i)}\right)$;
14. end for
15. Update $q_{k|k}$ using (10);
16. Update weight of particle $\hat{\mathbf{w}}_k^{(i)}$:
    $\hat{\mathbf{w}}_k^{(i)} = \frac{\mathbf{w}_{k|k-1}^{(i)}}{1-\Delta_k}\left(1 - p_D\left(\mathbf{x}_k\right) + p_D\left(\mathbf{x}_k\right)\sum_{m=1}^{|\mathbf{Z}_k|}\frac{g_k\left(\mathbf{z}_m|\mathbf{x}_k\right)}{\lambda c(\mathbf{z}_m)}\right)$;
17. Normalize weight $\bar{\mathbf{w}}_k^{(i)}$: $\bar{\mathbf{w}}_k^{(i)} = \hat{\mathbf{w}}_k^{(i)}/N_k$;
18. Resampling $N_k$ times from $\left\{\mathbf{x}_{k|k-1}^{(i)}, \bar{\mathbf{w}}_k^{(i)}\right\}_{i=1}^{N_k}$ to obtain particle set $\left\{\mathbf{x}_k^{(i)}, \mathbf{w}_k^{(i)}\right\}_{i=1}^{N_k}$, where $\mathbf{w}_k^{(i)} = 1/N_k$;
19. Compute $s_{k|k}(\mathbf{x}_k)$ using (13);

**Output:**

20. Report $q_{k|k}$, $s_{k|k}(\mathbf{x}_k)$ and $\left\{\mathbf{x}_k^{(i)}, \mathbf{w}_k^{(i)}\right\}$.

## 4. AUXILIARY PARTICLE BERNOULLI FILTER

Since the weight can reflect the ability of particles to explain the measurement [20, 27], the proposed filter will select the promising particles to propagate by drawing particle indices from a discrete distribution of particle set. At the same time, the particles without significant contribution to the approximation of probability density are discarded immediately.

### 4.1. Filtering principle

Drawing on the basic ideas from the AP method, we first extend the particle set $\left\{\mathbf{x}_{k-1}^{(i)}, \mathbf{w}_{k-1}^{(i)}\right\}_{i=1}^{N_{k-1}}$ and insert an extra particle $\mathbf{x}_{k-1}^{(N_{k-1}+1)}$ and its weight $\mathbf{w}_{k-1}^{(N_{k-1}+1)}$ based on the statistical characteristics:

$$\mathbf{w}_{k-1}^{(N_{k-1}+1)} = \int b_{k|k-1}\left(\mathbf{x}_k\right)\mathrm{d}\mathbf{x}_k, \tag{14}$$

$$f_{k-1}\left(\mathbf{x}_k|\mathbf{x}_{k-1}^{(N_{k-1}+1)}\right) = \frac{1-q_{k-1|k-1}}{q_{k-1|k-1}}\frac{b_{k|k-1}\left(\mathbf{x}_k\right)}{\mathbf{w}_{k-1}^{(N_{k-1}+1)}}, \tag{15}$$

$$p_{s,k|k-1}\left(\mathbf{x}_{k-1}^{(N_{k-1}+1)}\right) = 1. \tag{16}$$

Note that $\mathbf{x}_{k-1}^{(N_{k-1}+1)}$ is assigned to any point in $\mathcal{X}$ owing to its irrelevant in the higher dimensional space $\mathcal{X} \times \{1,\cdots,N_{k-1}+1\} \times \{1,\cdots,|\mathbf{Z}_k|\}$. Subsequently, we define the test function $\varphi(\cdot)$, whose integral in $\mathcal{X}$ at time $k$ is given by the following equation:

$$\begin{aligned}
&\int_{\mathcal{X}} \phi\left(\mathbf{x}_k\right) s_{k|k}\left(\mathbf{x}_k\right)\mathrm{d}\mathbf{x}_k \\
&= \sum_{m=1}^{|\mathbf{Z}_k|}\sum_{i=1}^{N_{k-1}+1}\int_{\mathcal{X}} \phi\left(\mathbf{x}_k\right)\frac{q_{k-1|k-1}p_D\left(\mathbf{x}_k\right)}{q_{k|k-1}\left(1-\Delta_{k,m}\right)}\frac{g_k\left(\mathbf{z}_m|\mathbf{x}_k\right)}{\lambda c\left(\mathbf{z}_m\right)} \\
&\quad\times \frac{p_{s,k|k-1}\left(\mathbf{x}_{k-1}^{(i)}\right) f_{k|k-1}\left(\mathbf{x}_k|\mathbf{x}_{k-1}^{(i)}\right)\mathbf{w}_{k-1}^{(i)}}{\pi_1\left(\mathbf{x}_k, \mathbf{x}_{k-1}^{(i)}, m\right)} \\
&\quad\times \delta_{\mathbf{x}_{k-1}^{(i)}}\left(\mathrm{d}\mathbf{x}_{k-1}\right)\pi_1\left(\mathrm{d}\mathbf{x}_k, \mathbf{x}_{k-1}^{(i)}, m\right) \\
&\quad+ \sum_{i=1}^{N_{k-1}+1}\int_{\mathcal{X}} \phi\left(\mathbf{x}_k\right)\frac{q_{k-1|k-1}\left(1-p_D\left(\mathbf{x}_k\right)\right)}{q_{k|k-1}\left(1-\Delta_{k,m}\right)} \\
&\quad\times \frac{p_{s,k|k-1}\left(\mathbf{x}_{k-1}^{(i)}\right) f_{k|k-1}\left(\mathbf{x}_k|\mathbf{x}_{k-1}^{(i)}\right)\mathbf{w}_{k-1}^{(i)}}{\pi_2\left(\mathbf{x}_k, \mathbf{x}_{k-1}^{(i)}\right)} \\
&\quad\times \delta_{\mathbf{x}_{k-1}^{(i)}}\left(\mathrm{d}\mathbf{x}_{k-1}\right)\pi_2\left(\mathrm{d}\mathbf{x}_k, \mathbf{x}_{k-1}^{(i)}\right).
\end{aligned} \tag{17}$$

We have in hand the card parameter $\Upsilon_{n,u} = \{i \in \{1,2,\cdots, N_{k-1}\} : m_n^{(i)} = u\}$ and $N_m = \#\Upsilon_{n,m}$, where $\#(\cdot)$ denotes the ordinal operation, and $\Delta_{k,m}$ is:

$$\Delta_{k,m} = \frac{p_D\left(\mathbf{x}_k\right)}{N_m}\left(1 - \sum_{i\in\Upsilon_{n,m}}\left(\begin{array}{l}\frac{g_k\left(z_m|\mathbf{x}_k\right)}{\lambda c\left(z_m\right)}\frac{q_{k-1|k-1}}{q_{k|k-1}} \\ \times\, p_{s,k|k-1}\left(\mathbf{x}_{k-1}^{(i)}\right) \\ \times\, f_{k|k-1}\left(\mathbf{x}_k|\mathbf{x}_{k-1}^{(i)}\right)\mathbf{w}_{k-1}^{(i)}\end{array}\right)\right). \tag{18}$$

Given that the proposal distribution $\pi_1\left(\mathbf{x}_k,\mathbf{x}_{k-1}^{(i)},m\right)$ can be extended to the higher dimension space of the detected targets, we can factorize it as follows:

$$\pi_1\left(\mathbf{x}_k,\mathbf{x}_{k-1}^{(i)},m\right)=\pi_1\left(\mathbf{x}_k|\mathbf{x}_{k-1}^{(i)},m\right)\pi_1\left(\mathbf{x}_{k-1}^{(i)}|m\right)\pi_1(m), \tag{19}$$

where

$$\pi_1\left(\mathbf{x}_k|\mathbf{x}_{k-1}^{(i)},m\right)=\mathrm{N}\left(\mathbf{x}_k|\mu_{k|k,1},\sigma_{k|k,1}^2\right), \tag{20}$$

$$\pi_1\left(\mathbf{x}_{k-1}^{(i)}|m\right)=\frac{\sum_{i=1}^{N_{k-1}+1}\gamma_1\left(\mathbf{x}_{k-1}^{(i)}\right)\mathbf{w}_{k-1}^{(i)}\delta_{\mathbf{x}_{k-1}^{(i)}}(\mathbf{x}_{k-1})}{\sum_{i=1}^{N_{k-1}+1}\gamma_1\left(\mathbf{x}_{k-1}^{(i)}\right)\mathbf{w}_{k-1}^{(i)}}, \tag{21}$$

$$\begin{aligned}\pi_1(m)&=\frac{q_{k-1|k-1}}{\left(1-\Delta_k^{N_{k-1}}\right)q_{k|k-1}}\frac{\sum_{i=1}^{N_{k-1}+1}\gamma_1\left(\mathbf{x}_{k-1}^{(i)}\right)\mathbf{w}_{k-1}^{(i)}}{\lambda c(z_m)}\\&\propto\frac{\sum_{i=1}^{N_{k-1}+1}\gamma_1\left(\mathbf{x}_{k-1}^{(i)}\right)\mathbf{w}_{k-1}^{(i)}}{\lambda c(z_m)}.\end{aligned} \tag{22}$$

In (20), $\pi_1\left(\mathbf{x}_k|\mathbf{x}_{k-1}^{(i)},m\right)$ follows the Gaussian distribution $\mathrm{N}\left(\mathbf{x}_k|\mu_{k|k,1},\sigma_{k|k,1}^2\right)$, where $\mu_{k|k,1}$ and $\sigma_{k|k,1}^2$ are the mean vector and covariance matrix. Further, the bounded potential function $\gamma_1\left(\mathbf{x}_{k-1}^{(i)}\right)$ is:

$$\gamma_1\left(\mathbf{x}_{k-1}^{(i)}\right)=\int_{\mathcal{X}}\left(\begin{array}{l}p_D(\mathbf{x}_k)\,g_k(z_m|\mathbf{x}_k)\,p_{s,k|k-1}\left(\mathbf{x}_{k-1}^{(i)}\right)\\\times f_{k|k-1}\left(\mathbf{x}_k|\mathbf{x}_{k-1}^{(i)}\right)\end{array}\right)\mathrm{d}\mathbf{x}_k. \tag{23}$$

Similarly, the proposal distribution $\pi_2\left(\mathbf{x}_k,\mathbf{x}_{k-1}^{(i)}\right)$ can be extended to the higher dimension space of the undetected targets, which can be factorized as:

$$\pi_2\left(\mathbf{x}_k,\mathbf{x}_{k-1}^{(i)}\right)=\pi_2\left(\mathbf{x}_k|\mathbf{x}_{k-1}^{(i)}\right)\pi_2\left(\mathbf{x}_{k-1}^{(i)}\right), \tag{24}$$

where

$$\pi_2\left(\mathbf{x}_k|\mathbf{x}_{k-1}^{(i)}\right)=\mathrm{N}\left(\mathbf{x}_k|\mu_{k|k,2},\sigma_{k|k,2}^2\right), \tag{25}$$

$$\begin{aligned}\pi_2\left(\mathbf{x}_{k-1}^{(i)}\right)&=\frac{q_{k-1|k-1}}{(1-\Delta_{k,m})q_{k|k-1}}\\&\quad\times\frac{\sum_{i=1}^{N_{k-1}+1}\gamma_2\left(\mathbf{x}_{k-1}^{(i)}\right)\mathbf{w}_{k-1}^{(i)}\delta_{\mathbf{x}_{k-1}^{(i)}}(\mathbf{x}_{k-1})}{\sum_{i=1}^{N_{k-1}+1}\gamma_2\left(\mathbf{x}_{k-1}^{(i)}\right)\mathbf{w}_{k-1}^{(i)}}\\&\propto\frac{\sum_{i=1}^{N_{k-1}+1}\gamma_2\left(\mathbf{x}_{k-1}^{(i)}\right)\mathbf{w}_{k-1}^{(i)}\delta_{\mathbf{x}_{k-1}^{(i)}}(\mathbf{x}_{k-1})}{\sum_{i=1}^{N_{k-1}+1}\gamma_2\left(\mathbf{x}_{k-1}^{(i)}\right)\mathbf{w}_{k-1}^{(i)}}.\end{aligned} \tag{26}$$

In (25), we note that $\pi_2\left(\mathbf{x}_k|\mathbf{x}_{k-1}^{(i)}\right)$ follows the Gaussian distribution $\mathrm{N}\left(\mathbf{x}_k|\mu_{k|k,2},\sigma_{k|k,2}^2\right)$, and the bounded potential function $\gamma_2\left(\mathbf{x}_{k-1}^{(i)}\right)$ in (26) can be written as:

$$\gamma_2\left(\mathbf{x}_{k-1}^{(i)}\right)=\int_{\mathcal{X}}\left(\begin{array}{l}(1-p_D(\mathbf{x}_k))\,p_{s,k|k-1}\left(\mathbf{x}_{k-1}^{(i)}\right)\\\times f_{k|k-1}\left(\mathbf{x}_k|\mathbf{x}_{k-1}^{(i)}\right)\end{array}\right)\mathrm{d}\mathbf{x}_k. \tag{27}$$

In (19) and (24), we can draw $N_{k-1,1}$ independent, identically distribution (IID) samples $\left\{\mathbf{x}_{k,1}^{(n)},\mathbf{x}_{k-1,1}^{(i_n)},m^{(n)}\right\}$ from $\pi_1\left(\mathbf{x}_k,\mathbf{x}_{k-1}^{(i)},m\right)$ and $N_{k-1,2}$ IID samples $\left\{\mathbf{x}_{k,2}^{(l)},\mathbf{x}_{k-1,2}^{(i_l)}\right\}$ from $\pi_2\left(\mathbf{x}_k,\mathbf{x}_{k-1}^{(i)}\right)$, where $i_n$ and $i_l$ denote the parent indices of the $n$th particle and the $l$th particle respectively. Then, the important weights according to them can be rewritten as:

$$\begin{aligned}&\mathbf{w}_{k,1}\left(\mathbf{x}_{k,1}^{(n)},\mathbf{x}_{k-1,1}^{(i_n)},m^{(n)}\right)\\&=\frac{1}{N_{k-1,1}}\frac{q_{k-1|k-1}}{\left(1-\Delta_{k,m}\right)q_{k|k-1}}\frac{g_k\left(z_{m^{(n)}}|\mathbf{x}_{k,1}^{(n)}\right)}{\lambda c\left(z_{m^{(n)}}\right)}\\&\quad\times\frac{p_D\left(\mathbf{x}_{k,1}^{(n)}\right)p_{s,k|k-1}\left(\mathbf{x}_{k-1,1}^{(i_n)}\right)f_{k|k-1}\left(\mathbf{x}_{k,1}^{(n)}|\mathbf{x}_{k-1,1}^{(i_n)}\right)\mathbf{w}_{k-1}^{(i_n)}}{\pi_1\left(\mathbf{x}_{k,1}^{(n)},\mathbf{x}_{k-1,1}^{(i_n)},m^{(n)}\right)},\end{aligned} \tag{28}$$

$$\begin{aligned}&\mathbf{w}_{k,2}\left(\mathbf{x}_{k,2}^{(l)},\mathbf{x}_{k-1,2}^{(i_l)}\right)\\&=\frac{1}{N_{k-1,2}}\frac{q_{k-1|k-1}}{\left(1-\Delta_{k,m}\right)q_{k|k-1}}\\&\quad\times\frac{1}{\pi_1\left(\mathbf{x}_{k,2}^{(l)},\mathbf{x}_{k-1,2}^{(i_l)}\right)}\left(\left(1-p_D\left(\mathbf{x}_{k,2}^{(l)}\right)\right)p_{s,k|k-1}\left(\mathbf{x}_{k-1,2}^{(i_l)}\right)\right.\\&\quad\left.\times f_{k|k-1}\left(\mathbf{x}_{k,2}^{(l)}|\mathbf{x}_{k-1,2}^{(i_l)}\right)\mathbf{w}_{k-1}^{(i_l)}\right).\end{aligned} \tag{29}$$

**Remark 4:** In the special case of the linear dynamics with the Gaussian perturbations, the Kalman filter (KF) is used as an optimal estimator. However, for the nonlinear dynamics, the KF is difficult because the state estimation is infinite dimensional. In general, a truncation is performed to arrive at the finite dimensional designs, where the UT is the most popular method that has been applied in the nonlinear systems. In this note, we employ the UT method to capture the posterior mean vector and covariance matrix for any nonlinearity in the AP-Bernoulli filter for the maneuvering target tracking:

$$\gamma_1\left(\mathbf{x}_{k-1}^{(i)}\right)=p_{s,k|k-1}\left(\mathbf{x}_{k-1}^{(i)}\right)\sum_{j=1}^{r}\varepsilon_{k,j}p_D(\chi_{k,j})\,g_k(z_m|\chi_{k,j}), \tag{30}$$

$$\gamma_2\left(\mathbf{x}_{k-1}^{(i)}\right)=p_{S,k|k-1}\left(\mathbf{x}_{k-1}^{(i)}\right)\sum_{j=1}^{r}\varepsilon_{k,j}\left(1-p_D(\chi_{k,j})\right), \tag{31}$$

where the UT can pick a minimal set of the sigma points $\{\chi_{k,j}\}_{j=1}^{r}$ and their weights $\{\varepsilon_{k,j}\}_{j=1}^{r}$ around the mean vector and the covariance matrix of $f_{k|k-1}\left(\mathbf{x}_k|\mathbf{x}_{k-1}^{(i)}\right)$.

### 4.2. Particle implementation

Algorithm 2 presents the implementation of proposed filter. In time update, Steps 3-9 describe selection of discrete distribution when $N_{k-1,1}$ particles are drawn. After $\gamma_1\left(\mathbf{x}_{k-1}^{(i)}\right)$ is computed, we can obtain the particles $\mathbf{x}_{k,1}^{(n)}$ and the related proposal distribution $\pi_1\left(\mathbf{x}_{k,1}^{(n)},\mathbf{x}_{k-1,1}^{(i_n)},m^{(n)}\right)$. Similarly, the particles $\mathbf{x}_{k,2}^{(l)}$ and the related proposal distributions $\pi_2\left(\mathbf{x}_{k,2}^{(l)},\mathbf{x}_{k-1,2}^{(i_l)}\right)$ are achieved in steps 10∼15 based on $\gamma_2\left(\mathbf{x}_{k-1}^{(i)}\right)$. We have in hand $\Delta_{k,m}$ in measurement update, and then estimate $q_{k|k}$ using $m$ measurements. In step 20, we get the important weights of detected targets $\left\{\mathbf{w}_{k,1}\left(\mathbf{x}_{k,1}^{(n)},\mathbf{x}_{k-1,1}^{(i_n)},m^{(n)}\right)\right\}_{n=1}^{N_{k-11}}$ that are expressed by $\pi_1\left(\mathbf{x}_{k,1}^{(n)},\mathbf{x}_{k-1,1}^{(i_n)},m^{(n)}\right)$. Further, the ESS is used as a measure of performance of important weights. As a simple method to capture effect of variance inflations [19], the ESS can reach the maximal value that equals to total number of sampling particles, that is:

$$N_{\text{eff}}=\frac{1}{\sum_{i=1}^{N_k}\left(\mathbf{w}_k^{(i)}\right)^2} \tag{32}$$

In Step 22, we select the minimal validate between $N_{\text{eff},k,1}$ and $N_{k-1,1}$ as $N_{k,1}$. The same method is applied for computing the weights defined by undetected targets. Then, $\left\{\mathbf{w}_{k,2}\left(\mathbf{x}_{k,2}^{(l)},\mathbf{x}_{k-1,2}^{(i_l)}\right)\right\}_{l=1}^{N_{k2}}$ and $N_{k,2}$ are computed in Steps 23-25, and $s_{k|k}(\mathbf{x}_k)$ can be obtained in Step 27.

## 5. SIMULATIOM RESULTS AND DISCUSSIONS

In the numerical study, two typical scenarios are performed to validate the tracking performance of the proposed filter. The experimental environment was: Intel™ Core™ i5, 4 GB memory and MATLAB™ V8.0.

The target moves in a 2-dimension surveillance region $[-2000,2000]\times[0,2000]$ m$^2$, and the passive sensor is located on $(0,0)$ m with the probability of detection $P_D=98\%$. Two scenarios of different motions of a target during the whole period are simulated, where the duration is 100 s and the sampling period is $T=1$ s. The clutter is modeled as the Poisson distribution with uniform density in the surveillance region. Meanwhile, the averaged number of clutters returns per scan is 20. At each time, 250 particles are sampled, with 100 being assigned to $N_{b,0}$ in standard filter. For the proposed filter, $N_{0,2}$ is set to 50. Finally, the optimal subpattern assignment (OSPA) distance is used to measure two filters. Let $X=\{\mathbf{x}_i\}_{i=1}^{g}$ be the ground truth track set and let $\hat{X}=\{\hat{x}_i\}_{i=1}^{e}$ be the estimated track set, then the OSPA distance is usually given by the following

**Algorithm 2:** Pseudo-code of proposed Bernoulli filter

**Input:**

1. Given $q_{k-1|k-1}$, $\left\{\mathbf{x}_{k-1}^{(i)},\mathbf{w}_{k-1}^{(i)}\right\}_{i=1}^{N_{k-1}}$, $\mathbf{Z}_{k-1}$ and $\mathbf{Z}_k$;

**Time update:**

2. Compute $q_{k|k-1}$: $q_{k|k-1}=p_{b,k|k-1}\left(1-p_{k-1|k-1}\right)+p_{s,k|k-1}\left(\mathbf{x}_{k-1}^{(i)}\right)q_{k-1|k-1}$;
3. for $n=1$ to $N_{k-1,1}$
4. Compute $\gamma_1\left(\mathbf{x}_{k-1}^{(i)}\right)$ using (23);
5. Draw $m^{(n)}\sim\pi_1(m)$ using (22);
6. Draw $\mathbf{x}_{k-1,1}^{(i_n)}\sim\pi_1\left(\mathbf{x}_{k-1}|m^{(n)}\right)$ using (21);
7. Draw $\mathbf{x}_{k,1}^{(n)}\sim\pi_1\left(\mathbf{x}_k|\mathbf{x}_{k-1,1}^{(i_n)},m^{(n)}\right)$ using (20);
8. Compute $\pi_1\left(\mathbf{x}_{k,1}^{(n)},\mathbf{x}_{k-1,1}^{(i_n)},m^{(n)}\right)$ using (19);
9. end for
10. for $l=1$ to $N_{k-1,2}$
11. Compute $\gamma_2\left(\mathbf{x}_{k-1}^{(i)}\right)$ using (27);
12. Draw $\mathbf{x}_{k-1,2}^{(i_l)}\sim\pi_2(\mathbf{x}_{k-1})$ using (26);
13. Draw $\mathbf{x}_{k,2}^{(l)}\sim\pi_2\left(\mathbf{x}_k|\mathbf{x}_{k-1,2}^{(i_l)}\right)$ using (25);
14. Compute $\pi_2\left(\mathbf{x}_{k,2}^{(l)},\mathbf{x}_{k-1,2}^{(i_l)}\right)$ using (24);
15. end for

**Measurement update:**

16. for $m=1$ to $|\mathbf{Z}_k|$
17. Compute $\Delta_{k,m}$ using (18);
18. end for
19. Compute $q_{k|k}$: $q_{k|k}=\sum_{m=1}^{|\mathbf{Z}_k|}\frac{q_{k|k-1}-q_{k|k-1}\Delta_{k,m}}{1-q_{k|k-1}\Delta_{k,m}}$;
20. Compute $\left\{\mathbf{w}_{k,1}\left(\mathbf{x}_{k,1}^{(n)},\mathbf{x}_{k-1,1}^{(i_n)},m^{(n)}\right)\right\}_{n=1}^{N_{k-11}}$ using (28);
21. Compute $N_{\text{eff},k,1}$ using (32);
22. Compute $N_{k,1}$: $N_{k,1}=\min\left(N_{\text{eff},k,1},N_{k-1,1}\right)$;
23. Compute $\left\{\mathbf{w}_{k,2}\left(\mathbf{x}_{k,2}^{(l)},\mathbf{x}_{k-1,2}^{(i_l)}\right)\right\}_{l=1}^{N_{k2}}$ using (29);
24. Compute $N_{\text{eff},k,2}$ using (32);
25. Compute $N_{k,2}$: $N_{k,2}=\min\left(N_{\text{eff},k,2},N_{k-1,2}\right)$;
26. Select $N_{k,1}$ and $N_{k,2}$ particles based on their weights in a descending order, let $N_k=N_{k1}+N_{k2}$ and union of particles:
$$\left\{\mathbf{x}_k^{(i)},\mathbf{w}_k^{(i)}\right\}_{i=1}^{N_k}=\left\{\mathbf{w}_{k,1}\left(\mathbf{x}_{k,1}^{(n)},\mathbf{x}_{k-1,1}^{(i_n)},m^{(n)}\right),\mathbf{x}_{k,1}^{(n)}\right\}_{n=1}^{N_{k1}}\bigcup\left\{\mathbf{w}_{k,2}\left(\mathbf{x}_{k,2}^{(l)},\mathbf{x}_{k-1,2}^{(i_l)}\right),\mathbf{x}_{k,2}^{(l)}\right\}_{l=1}^{N_{k2}};$$
27. Compute $s_{k|k}(\mathbf{x}_k)$ using (13);

**Output:**

28. Report $q_{k|k}$, $s_{k|k}(\mathbf{x}_k)$ and $\left\{\mathbf{x}_k^{(i)},\mathbf{w}_k^{(i)}\right\}_{i=1}^{N_k}$.

equation:

$$\bar{d}_p^{(c)}\left(X,\hat{X}\right)=\begin{cases}\left(\frac{1}{\left|\hat{X}\right|}\left(\min\limits_{\pi\in\Pi_{\left|\hat{X}\right|}}\sum\limits_{i=1}^{|X|}d^{(c)}\left(\mathbf{x}_i,\hat{x}_{\pi(i)}\right)^p\right)\right)^{1/p}, & \\ \quad +c^p\left(\left|\hat{X}\right|-|X|\right) & |X|\le\left|\hat{X}\right|, \\ \min\left(c,\|x-\hat{x}\|\right), & \\ & |X|>\left|\hat{X}\right|, \end{cases} \tag{33}$$

where $\Pi_{\left|\hat{X}\right|}$ is the set of permutations in $\left|\hat{X}\right|$, $c$ is the cut-off parameter that determines the sensitivity of divergence from the cardinality error, $p$is the order parameter that determines sensitivity of the localization error. Here, we set $p=2$ and $c=70$ m.

### 5.1. Scenario 1: CV motion model

In this scenario, the target keeps a CV motion of velocity $(10,20)$ m s$^{-1}$ for 60 s from the initial position $(120,230)$ m on the 21st s. We use the state matrix $\mathbf{x}_k=[\mathbf{x}_k,\dot{x}_k,y_k,\dot{y}_k]^{\mathrm{T}}$ to represent the position $(\mathbf{x}_k,y_k)$ and the velocity $(\dot{x}_k,\dot{y}_k)$, where $[\cdot]^{\mathrm{T}}$denotes the transposed matrix. As for the CV motion model, the related matrices in (1) are further defined as follows:

$$F_{k|k-1}=\begin{bmatrix}1&1&0&0\\0&1&0&0\\0&0&1&1\\0&0&0&1\end{bmatrix}\text{ and }\Gamma_k=\begin{bmatrix}0.5&0\\1&0\\0&0.5\\0&1\end{bmatrix}.$$

Additionally, the target dynamics are observed based on the standard deviation diag(100,20,100,20). The standard deviation for the measurement noise is diag(0.0349,10) , where diag $(\cdot)$ denotes the diagonal matrix.

Fig. 1 demonstrates the track of the moving target and the related measurements in a dense clutter area under 100 Monte Carlo trials. It can be seen that the surveillance is a top half-disc of radius 2000 m. As expected, the track is a straight line that reflects the target with the CV motion throughout the surveillance time. In addition, it is obvious that the measurements become more concentrated around the passive sensor.

Fig. 2 illustrates the true track, measurements, and position estimates in both $x$ and $y$ coordinates during the 21st-80th s. Note that the position estimates of the proposed filter make a stealthy approach to the true position. The tracking performance of it is compared with that of the standard filter that subsumes many traditional tracking methods in clutter environments. Further, the standard filter based on the UT method tends to seriously drift off the true track and erroneously follows the position of extraneous clutter-generated measurements. However, the proposed filter correctly identifies the estimated position, which does not suffer from multi-measurements generated by clutters. Simultaneously, it inherently overcomes the defects of standard filter on the CV motion model.

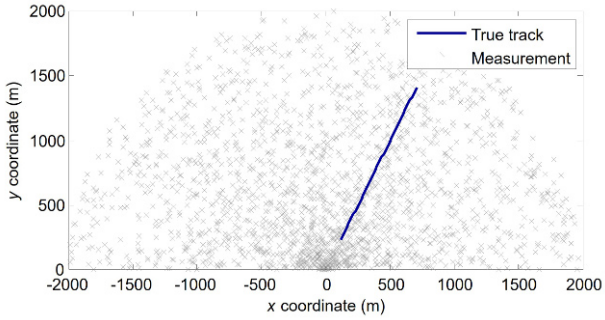


Fig. 1. Target track and measurements.

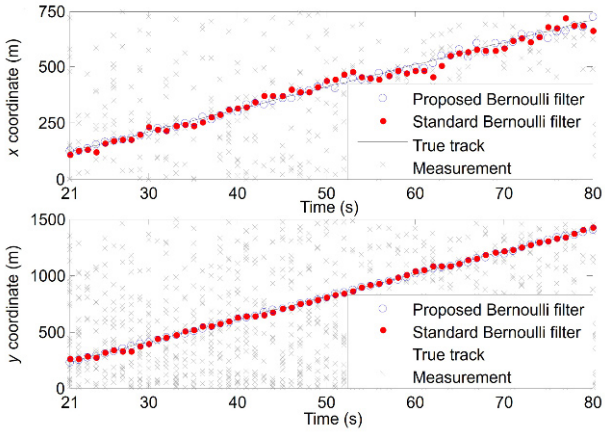


Fig. 2. Target state estimates.

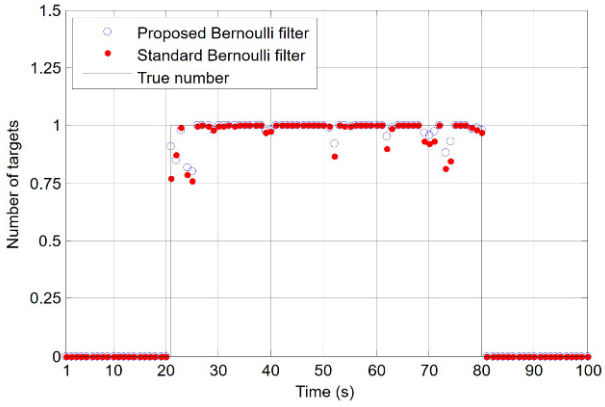


Fig. 3. Target number estimates.

In Fig. 3, the summary statistics of the cardinality estimates are shown. This figure reports both filters can converge to the ground truth number. The estimated number is not affected by heuristic clustering because it is made on the basis of total mass of the particle set. Note that the proposed filter adheres to its confidence in the number estimates with smaller variance.

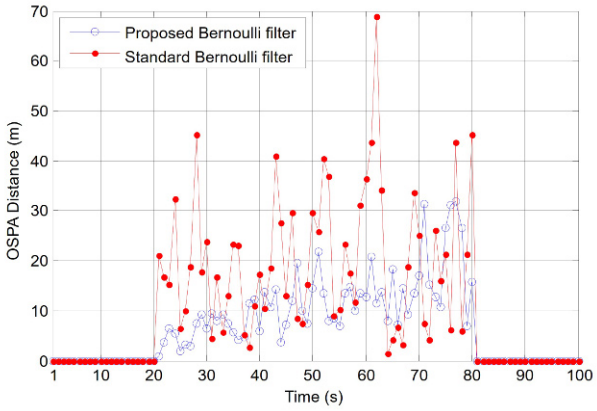


Fig. 4. OSPA distance.

Fig. 4 demonstrates the OSPA distance of two filters. In terms of the OSPA distance, the filters are penalized in the unequal amounts. The standard filter settles to the distance error consistent with the standard deviation of the measurement noise, whilst the proposed filter achieves the lower error as a direct result of always approaching the true position. Due to employing natural mechanism for obtaining state estimates, the proposed filter gives more advantage to the localization component.

### 5.2. Scenario 2: CT motion model

The maneuvering target executes an anticlock CT motion of velocity $(10,20)$ m s$^{-1}$ for 60 s from the initial position $(95,220)$ m on the 21st s. The state matrix is $\mathbf{x}_k = [x_k, \dot{x}_k, y_k, \dot{y}_k, \omega_k]^{\mathrm{T}}$, where the turn rate at time $k$ is $\omega_k = 0.02$ rad s$^{-1}$, the standard deviation of isotropic Gaussian noise is diag$\,(100, 10, 100, 10, 1)$, and the standard deviation for the measurement noise stays the same with Scenario 1. Then, the related matrices in (1) are given by:

$$F_{k|k-1} = \begin{bmatrix} 1 & 0.9999 & 0 & -0.0100 & 0 \\ 0 & 0.9998 & 0 & -0.0200 & 0 \\ 0 & 0.0100 & 1 & 0.9999 & 0 \\ 0 & 0.0200 & 0 & 0.9998 & 0 \\ 0 & 0 & 0 & 0 & 1 \end{bmatrix}$$

and

$$\Gamma_k = \begin{bmatrix} 0.5 & 0 & 0 \\ 1 & 0 & 0 \\ 0 & 0.5 & 0 \\ 0 & 1 & 0 \\ 0 & 0 & 1 \end{bmatrix}.$$

Fig. 5 shows the track of target and measurements. Note that the track is a curve in the top half-disc of the radius 2000 m, which means the target moves with the CT motion during the surveillance period. Simultaneously, a large number of measurements are randomly generated in the surveillance region.

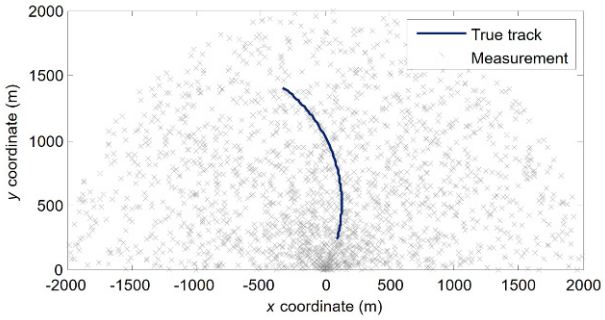


Fig. 5. Target track and measurements.

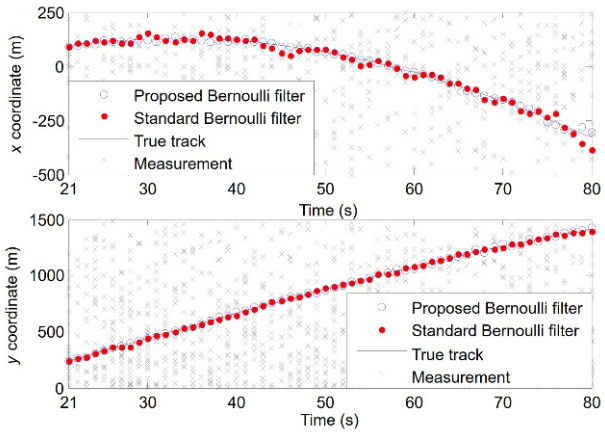


Fig. 6. Target state estimates.

In Fig. 6, the true track and the outputs of two filters are shown in both $x$ and $y$ coordinates during the 21st-80th s. The preliminary results suggest that the proposed filter is suitable for the maneuvering target tracking in the presence of clutters, whereas the standard filter has estimation bias. It is clear that the proposed filter provides a lower variance than the standard filter by propagating entire distribution.

The estimated number versus time is demonstrated in Fig. 7. As expected, it can be observed that the proposed filter produces results essentially in agreement with the ground truth number. On the contrary, the standard filter has unstable number estimates. The explanation is that the standard filter's number estimates have high variance with low confidence. Its estimates are easily influenced by new measurements especially when the target is moving with maneuvering dynamics.

Fig. 8 compares the OSPA distance of two filters. In this figure, we note that the OSPA distance of the proposed filter during the whole surveillance period is lower than that of the standard filter. The results indicate a dramatic improvement in tracking accuracy. Many particles

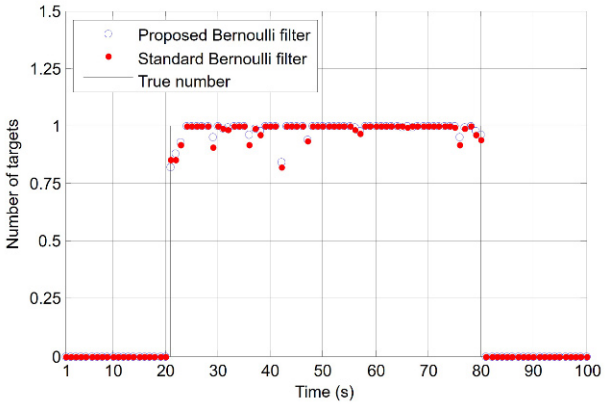


Fig. 7. Target number estimates.

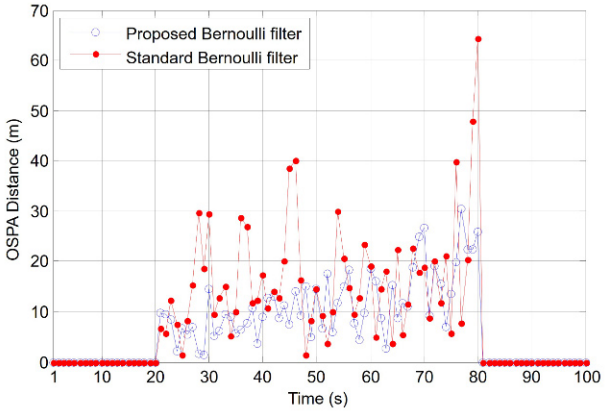


Fig. 8. OSPA distance.

Table 1. Comparison of tracking performance.

| | Target number | OSPA distance (m) | ESS (%) |
|---|---|---|---|
| Standard filter | 0.9806 | 17.5691 | 18.77 |
| Proposed filter | 0.9872 | 11.6870 | 62.02 |

concentrate on the target when employing the UT scheme. In view of the OSPA distance sensitive to the localization error, the improvement derives mainly from the reduction in the localization error.

Finally, Table 1 shows the average comparison results of two filters under 1000 Monte Carlo trials, where consists the time-averaged OSPA distance, estimated number and ESS during the 21st-80th s. In this table, it can be found that the proposed filter keeps perfect number estimates and saves 33.48% OSPA distance, which indicates the proposed filter boosts the accuracy of state estimation. Regarding the ESS, the standard filter has only 30.26% EES of the proposed filter. As a result, the OSPA distance of the standard filter is larger. The investigation further shows that two filters are roughly similar for the computational cost. Although it incurs extra costs related to computing the related parameters of the proposal distributions, the proposed filter consists of simply computing estimates from smaller number of particles by which measurements they are effectively assigned to, which also balances total costs by inexpensive scheme of the state estimates. From this table, we can conclude that the proposed filter has expected improvements.

## 6. CONCLUSION

This paper has developed an AP implementation of the Bernoulli filter. The challenges are to handle inefficient tracking and imprecise estimates of the standard Bernoulli filter in noisy set of measurements. Our work employs the AP method to minimize the variance of the important weight in order to obtain low variance estimates. Moreover, the AP method provides guidance on selection of the proposal distributions using the potential particles. Afterwards, the famous UT scheme further implements the maneuvering target tracking. The numerical study shows that the AP-Bernoulli filter has remarkable improvement in the tracking performance with promising results. As the future developments of this work, we will shorten running time under the current tracking accuracy.

## REFERENCES

[1] S. S. Blackman and R. F. Popoli, *Design and Analysis of Modern Tracking Systems*, Aretch House, Norwood, 1999.

[2] R. Mahler, *Statistical Multisource Multitarget Information Fusion*, Aretch House, Norwood, 2007.

[3] P. S. Maybeck, *Stochastic Models, Estimation, and Control*, Academic Press, Salt Lake City, 1982.

[4] Y. Bar-Shalom, *Multitarget-Multisensor Tracking: Applications and Advances*, Aretch House, Norwood, 1992.

[5] B. Li, "Multiple-model Rao-Blackwellized particle particle probability hypothesis density filter for multitarget tracking," *International Journal of Control, Automation and Systems*, vol. 13, no. 2, pp. 426-433, April 2015. [click]

[6] D. Musicki, R. Evans, and S. Stankovic, "Integrated probabilistic data association," *IEEE Trans. on Automatic Control*, vol. 39, no. 6, pp. 1237-1241, June 1994. [click]

[7] D. Musicki and R. Evans, "Joint integrated probabilistic data association-JIPDA," *IEEE Trans. on Aerospace and Electronic Systems*, vol. 40, no. 3, pp. 1093-1099, July 2004. [click]

[8] S. S. Blackman, "Multiple hypotheses tracking for multiple target tracking," *IEEE Aerospace Electronic Systems Magazine*, vol. 19, no. 1, pp. 5-18, January 2004. [click]

[9] R. Mahler, *Advances in Statistical Multisource Multitarget Information Fusion*, Aretch House, Norwood, 2014.

[10] B. T. Vo, *Random Finite Sets in Multi-Object Filtering*, The University of Western Australia, Perth 2008.

[11] B. T. Vo, D. Clark, B. N. Vo, and B. Ristic, "Bernoulli forward-backward smoothing for joint target detection and tracking," *IEEE Trans. on Signal Processing*, vol. 59, no. 9, pp. 4473-4477, September 2011. [click]

[12] B. Ristic and S. Arulampalam, "Bernoulli particle filter with observer control for bearings only tracking in clutter," *IEEE Trans. on Aerospace and Electronic Systems*, vol. 48, no. 7, pp. 2405-2415, July 2012. [click]

[13] A. Gning, B. Ristic, and L. Mihaylova, "Bernoulli particle/box-particle filters for detection and tracking in the presence of triple measurement uncertainty," *IEEE Trans. on Signal Processing*, vol. 60, no. 2, pp. 2138-2151, May 2012. [click]

[14] B. T. Vo, C. See, N. Ma, and W. Ng, "Multi-sensor joint detection and tracking with the Bernoulli filter," *IEEE Trans. on Aerospace and Electronic Systems*, vol. 48, no. 2, pp. 1385-1402, April 2012. [click]

[15] B. T. Vo, B. N. Vo, and A. Cantoni, "The cardinality balanced multi-target multi-Bernoulli filter and its implementation," *IEEE Trans. on Signal Processing*, vol. 57, no. 2, pp. 409-423, February 2009. [click]

[16] X. B. Luo, H. Q. Fan, Z. Y. Song, and Q. Fu, "Bernoulli particle filter with observer altitude for maritime radiation source tracking in the presence of measurement uncertainty," *Chinese Journal of Aeronautics*, vol. 26, no. 6, pp. 1459-1470, December 2013. [click]

[17] B. Ristic, *Particle Filters for Random Set Models*, Springer, New York, 2013.

[18] B. T. Vo, B. N. Vo, and A. Farina, "A tutorial on Bernoulli filters: theory, implementation and applications," *IEEE Trans. on Signal Processing*, vol. 61, no. 13, pp. 3406-3430, July 2013. [click]

[19] L. Ubeda-Medina, A. F. Garcia-Fernandez, and J. Grajal, Generalization of the auxiliary particle filter for multiple target tracking, *Proc. of the 17th International Conference on Information Fusion*, Salamanca, pp. 1-8, 2014.

[20] N. Whiteley, S. Singh, and S. Godsill, "Auxiliary particle implementation of probability hypothesis density filter," *IEEE Trans. on Aerospace and Electronic Systems*, vol. 46, no. 3, pp. 1437-1454, July 2010. [click]

[21] M. R. Danaee and F. Behnia, Auxiliary unscented particle cardinalized probability hypothesis density, *Proc. of the 21st Iranian Conference on Electrical Engineering,* Mashhad, pp. 1-6, 2013.

[22] H. Chen and G. Z. Han, "A new sequence Monte Carlo implementation of cardinality balanced multi-target multi-Bernoulli filter," *Acta Automatica Sinaca*, vol. 42, no.1, pp. 26-36, January 2016. [click]

[23] H. Qiu, G. M. Huang, and J. Gao, "Unscented particle implementation of cardinality balanced multi-target multi-Bernoulli filter," *Proc. of the 7th International Congress on Image and Signal Processing*, Dalian, pp. 1162-1166, 2014.

[24] S. C. Zhang, J. X. Li, and L .B. Wu, "A novel multiple maneuvering targets tracking algorithm with data association and track management," *International Journal of Control, Automation and Systems*, vol. 11, no.5, pp. 947-956, October 2013. [click]

[25] Z. Liu, S. Xu, Y. Zhang, X. Chen, and C. L. P. Chen, "Interval type-2 fuzzy kernel based support vector machine algorithm for scene classification of humanoid robot," *Soft Computing*, vol. 18, no. 3, pp. 589-606, March 2014. [click]

[26] C. H. Xv, Y. Liu, W. Xiong, R. H. Song, and T. M. Li, "A dual threshold particle PHD filter with unknown target birth intensity," *Acta Aeronautica et Astronautica Sinica*, vol. 36, no. 12, pp. 3957-3969, December 2015.

[27] E. Baser and M. Efe, "A novel auxiliary particle PHD filter," *Proc. of the 15th International Conference on Information Fusion*, Singapore, pp. 165-172, 2012.

**Bo Li** received the B.S. and Ph.D degrees in Communication and Information System from Liaoning University of Technology and Dalian Maritime University, China, in 2005 and 2015, respectively. He is an associate professor in Liaoning University of Technology, China. His research interests include information fusion, state estimate, target tracking, and digital signal processing.

**Jianli Zhao** is currently a B.S. candidate in Communication and Information System from Liaoning University of Technology, China. His research interests include target tracking, and state estimate, information fusion.